Supporting Information

Long lifetime phosphorescence and X-ray scintillation of chlorobismuthate hybrids incorporating ionic liquid cations

Jian-Ce Jin,[a,c] Yang-Peng Lin,[b] Yi-Heng Wu,[a,c] Liao-Kuo Gong,[a] Nan-Nan Shen,[a] Ying Song,[d] Wen Ma,[a] Zhi-Zhuan Zhang,[a,b] Ke-Zhao Du* [b] and Xiao-Ying Huang* [a]

[a.] State Key Laboratory of Structure Chemistry, Fujian Institute of Research on the Structure of Matter, Chinese Academy of Sciences, Fuzhou 350002, China.

[b.] College of Chemistry and Materials Science, Fujian Provincial Key Laboratory of Advanced Materials Oriented Chemical Engineering, Fujian Normal University, 32 Shangsan Road, Fuzhou 350007, China.

[c.] University of Chinese Academy of Sciences, Bejing, 100049, China.

[d.] College of Chemistry and Materials, Nanning Normal University, Nanning, 530001, China.

E-mail: xyhuang@fjirsm.ac.cn

E-mail: duke@fjnu.edu.cn

Table S1 Crystallographic data for compound **1**, **2** at 290 K and 100 K.

Compound	**1-290K**	**1-100K**	**2-290K**	**2-100K**
Empirical formula	$BiCl_4C_{16}H_{19}N_4O_2$	$BiCl_4C_{16}H_{19}N_4$	$BiCl_4C_{17}H_{21}N_4$	$BiCl_4C_{17}H_{21}N_4$
Formula Mass	650.13	650.13	664.16	664.16
Crystal system	orthorhombic	orthorhombic	orthorhombic	orthorhombic
Space group	*Pca*2$_1$	*Pca*2$_1$	*Pbca*	*Pbca*
a/Å	14.6969(12)	14.4947(7)	16.4032(6)	16.2874(6)
b/Å	9.1488(9)	9.0474(6)	16.4094(6)	16.3137(6)
c/Å	16.2644(12)	16.1935(7)	17.3812(7)	17.1361(7)
V/Å^3	2186.9(3)	2123.6(2)	4678.4(3)	4553.2(3)
Z	4	4	8	8
T/K	290(2)	100(2)	290(2)	100(2)
λ/Å	0.71073	0.71073	0.71073	0.71073
F(000)	1240	1240	2544	2544
ρ_{calcd}/g cm^{-3}	1.975	2.033	1.886	1.938
μ/mm^{-1}	8.569	8.825	8.014	8.234
Measured refls.	14023	18014	85265	69454
Independent refls.	5575	6679	6753	4013
No. of parameters	284	247	256	256
R_{int}	0.0364	0.0440	0.0582	0.0575
R_1 ($I > 2\sigma(I)$)[a]	0.0355	0.0371	0.0276	0.0205
$wR(F^2)$ ($I > 2\sigma(I)$)[b]	0.0637	0.0698	0.0536	0.0494
GOF	1.003	1.006	1.024	1.015

[a] $R_1 = \sum \| F_o | - | F_c \| / \sum | F_o |$, [b] $wR_2 = [\sum w(F_o^2 - F_c^2)^2 / \sum w(F_o^2)^2]^{1/2}$.

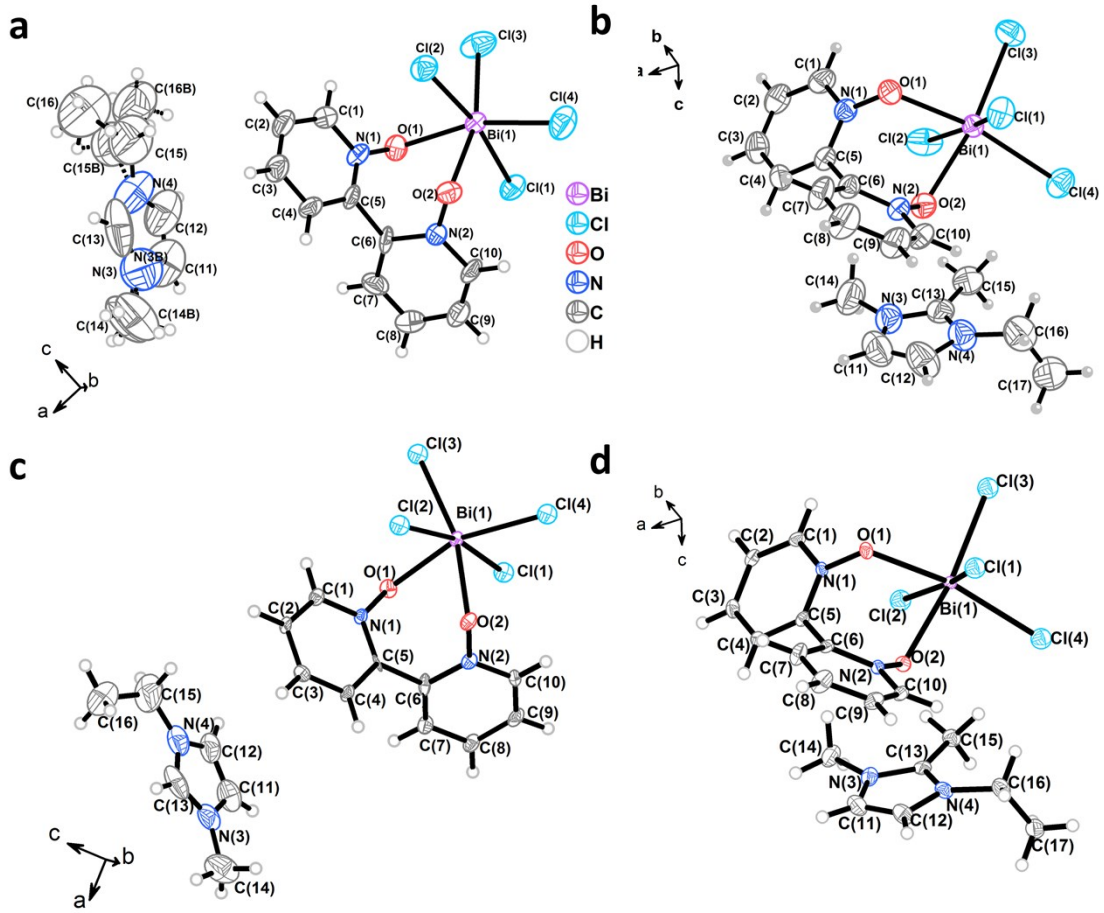

Fig. S1 *ORTEP* drawings (50% ellipsoid probability) of the asymmetric units of **1** at 290 K (a), at 100 K (c) and **2** at 290 K (b) and 100 K (d).

Table S2 Selected bond lengths (Å) and bond angles (°) for **1** and **2** at 290K and 100 K.

1 (290K)		**1 (100K)**	
Bi(1)−O(1)	2.405(7)	Bi(1)−O(1)	2.375(6)
Bi(1)−O(2)	2.389(8)	Bi(1)−O(2)	2.366(6)
Bi(1)−Cl(1)	2.650(3)	Bi(1)−Cl(1)	2.659(3)
Bi(1)−Cl(2)	2.690(3)	Bi(1)−Cl(2)	2.676(3)
Bi(1)−Cl(3)	2.694(4)	Bi(1)−Cl(3)	2.718(3)
Bi(1)−Cl(4)	2.704(4)	Bi(1)−Cl(4)	2.722(3)
O(1)−N(1)	1.309(11)	O(1)−N(1)	1.333(9)
O(2)−N(2)	1.344(12)	O(2)−N(2)	1.343(9)
N(3)−C(14)	1.434(13)	N(3)−C(14)	1.47(2)
N(4)−C(15)	1.424(12)	N(4)−C(15)	1.47(2)
C(15)−C(16)	1.44(2)	C(15)−C(16)	1.41(2)
N(4)−C(15B)	1.422(13)		
C(15B)−C(16B)	1.48(3)		
O(2)−Bi(1)−O(1)	74.7(2)	O(2)−Bi(1)−O(1)	75.52(17)
O(1)−Bi(1)−Cl(1)	83.52(19)	O(1)−Bi(1)−Cl(1)	81.97(15)
O(1)−Bi(1)−Cl(2)	87.9(2)	O(1)−Bi(1)−Cl(2)	87.84(17)

O(1)−Bi(1)−Cl(3)	89.2(2)	O(1)−Bi(1)−Cl(3)	89.91(17)
O(1)−Bi(1)−Cl(4)	162.2(2)	O(1)−Bi(1)−Cl(4)	160.77(18)
O(2)−Bi(1)−Cl(1)	88.7(2)	O(2)−Bi(1)−Cl(1)	88.00(17)
O(2)−Bi(1)−Cl(2)	83.6(2)	O(2)−Bi(1)−Cl(2)	82.61(15)
O(2)−Bi(1)−Cl(3)	163.5(2)	O(2)−Bi(1)−Cl(3)	164.82(18)
O(2)−Bi(1)−Cl(4)	88.1(2)	O(2)−Bi(1)−Cl(4)	86.06(17)
Cl(1)−Bi(1)−Cl(2)	169.70(7)	Cl(1)−Bi(1)−Cl(2)	167.61(5)
Cl(1)−Bi(1)−Cl(3)	93.35(10)	Cl(1)−Bi(1)−Cl(3)	94.25(7)
Cl(1)−Bi(1)−Cl(4)	91.48(12)	Cl(1)−Bi(1)−Cl(4)	92.05(11)
Cl(2)−Bi(1)−Cl(3)	92.23(12)	Cl(2)−Bi(1)−Cl(3)	92.76(11)
Cl(2)−Bi(1)−Cl(4)	95.00(10)	Cl(2)−Bi(1)−Cl(4)	95.34(7)
Cl(3)−Bi(1)−Cl(4)	108.22(12)	Cl(3)−Bi(1)−Cl(4)	108.83(9)
N(1)−O(1)−Bi(1)	118.4(6)	N(1)−O(1)−Bi(1)	117.6(5)
N(2)−O(2)−Bi(1)	115.5(6)	N(2)−O(2)−Bi(1)	116.7(5)
C(5)−N(1)−O(1)	121.8(12)	O(1)−N(1)−C(5)	119.6(9)
O(1)−N(1)−C(1)	119.4(10)	O(1)−N(1)−C(1)	118.8(7)
O(2)−N(2)−C(10)	119.2(10)	O(2)−N(2)−C(10)	118.9(7)
O(2)−N(2)−C(6)	118.0(13)	O(2)−N(2)−C(6)	119.8(10)
C(5)−N(1)−C(1)	118.8(13)	C(5)−N(1)−C(1)	121.6(9)
C(10)−N(2)−C(6)	122.6(14)	C(10)−N(2)−C(6)	121.2(10)
N(4)−C(15)−C(16)	125(3)	C(16)−C(15)−N(4)	115.6(18)
N(4)−C(15B)−C(16B)	121(3)		
2 (**290K**)		**2** (**100K**)	
Bi(1)−O(1)	2.419(3)	Bi(1)−O(1)	2.403(2)
Bi(1)−O(2)	2.406(3)	Bi(1)−O(2)	2.388(2)
Bi(1)−Cl(1)	2.6599(10)	Bi(1)−Cl(1)	2.6617(9)
Bi(1)−Cl(2)	2.6908(11)	Bi(1)−Cl(2)	2.6987(9)
Bi(1)−Cl(3)	2.6683(10)	Bi(1)−Cl(3)	2.6831(9)
Bi(1)−Cl(4)	2.6551(10)	Bi(1)−Cl(4)	2.6679(9)
O(1)−N(1)	1.331(4)	O(1)−N(1)	1.341(4)
O(2)−N(2)	1.329(4)	O(2)−N(2)	1.332(4)
N(3)−C(14)	1.461(6)	N(3)−C(14)	1.464(5)
N(4)−C(16)	1.493(6)	N(4)−C(16)	1.470(5)
C(13)−C(15)	1.465(6)	C(13)−C(15)	1.476(5)
C(16)−C(17)	1.464(8)	C(16)−C(17)	1.507(6)
O(2)−Bi(1)−O(1)	76.17(8)	O(2)−Bi(1)−O(1)	76.91(8)
O(1)−Bi(1)−Cl(1)	79.51(6)	O(1)−Bi(1)−Cl(1)	78.47(6)
O(1)−Bi(1)−Cl(2)	89.52(7)	O(1)−Bi(1)−Cl(2)	88.80(6)
O(1)−Bi(1)−Cl(3)	97.10(7)	O(1)−Bi(1)−Cl(3)	98.00(6)
O(1)−Bi(1)−Cl(4)	162.92(7)	O(1)−Bi(1)−Cl(4)	162.37(6)
O(2)−Bi(1)−Cl(1)	90.88(7)	O(2)−Bi(1)−Cl(1)	91.11(6)
O(2)−Bi(1)−Cl(2)	80.72(7)	O(2)−Bi(1)−Cl(2)	80.04(6)
O(2)−Bi(1)−Cl(3)	168.61(7)	O(2)−Bi(1)−Cl(3)	168.95(6)

O(2)−Bi(1)−Cl(4)	90.81(6)	O(2)−Bi(1)−Cl(4)	90.06(6)
Cl(1)−Bi(1)−Cl(2)	167.55(4)	Cl(1)−Bi(1)−Cl(2)	165.92(3)
Cl(1)−Bi(1)−Cl(3)	96.98(3)	Cl(1)−Bi(1)−Cl(3)	97.52(3)
Cl(3)−Bi(1)−Cl(2)	90.15(3)	Cl(3)−Bi(1)−Cl(2)	90.13(3)
Cl(4)−Bi(1)−Cl(1)	89.85(3)	Cl(1)−Bi(1)−Cl(4)	90.12(3)
Cl(4)−Bi(1)−Cl(2)	99.37(4)	Cl(4)−Bi(1)−Cl(2)	100.74(3)
Cl(4)−Bi(1)−Cl(3)	97.42(3)	Cl(4)−Bi(1)−Cl(3)	96.78(3)
N(1)−O(1)−Bi(1)	115.61(19)	N(1)−O(1)−Bi(1)	115.31(19)
N(2)−O(2)−Bi(1)	118.7(2)	N(2)−O(2)−Bi(1)	118.4(2)
O(1)−N(1)−C(1)	119.6(3)	O(1)−N(1)−C(1)	119.3(3)
O(1)−N(1)−C(5)	119.5(3)	O(1)−N(1)−C(5)	119.2(3)
O(2)−N(2)−C(6)	119.5(3)	O(2)−N(2)−C(6)	119.4(3)
O(2)−N(2)−C(10)	119.8(3)	O(2)−N(2)−C(10)	119.2(3)
C(1)−N(1)−C(5)	120.8(3)	C(1)−N(1)−C(5)	121.5(3)
C(10)−N(2)−C(6)	120.7(3)	C(10)−N(2)−C(6)	121.4(3)
C(17)−C(16)−N(4)	110.4(5)	N(4)−C(16)−C(17)	112.8(3)

Table S3 Hydrogen bonding data for **1** and **2** at 290K and 100K.

D−H···A	D−H (Å)	H···A (Å)	D···A (Å)	<(DHA) (°)
1-290 K				
H-bond in anions				
C(1)−H(1A)···Cl(1)#1	0.93	2.87	3.507(13)	126.6
C(2)−H(2A)···Cl(1)#1	0.93	2.94	3.53(3)	123.3
C(2)−H(2A)···Cl(4)#1	0.93	2.90	3.70(3)	145.0
C(4)−H(4A)···Cl(4)#2	0.93	2.90	3.624(12)	135.8
C(7)−H(7A)···Cl(1)#3	0.93	2.96	3.614(11)	128.9
C(7)−H(7A)···Cl(3)#3	0.93	2.83	3.588(14)	139.5
C(9)−H(9A)···Cl(3)#4	0.93	2.79	3.64(3)	152.5
C(10)−H(10A)···Cl(2)#4	0.93	2.83	3.501(11)	129.8
H-bonds between anions and cations				
C(11)−H(11A)···O(1)#3	0.93	2.58	3.393(19)	146.0
C(13)−H(13A)···Cl(4)#5	0.93	2.80	3.71(2)	166.0
C(14^a)−H(14B^a)···Cl(3)#6	0.96	2.66	3.60(6)	166.9
C(16^a)−H(16C^a)···O(2)#5	0.96	2.54	3.40(3)	149.3
C(14B^b)−H(14E^b)···Cl(3)#6	0.96	2.90	3.85(13)	172.7
C(15B^b)−H(15D^b)···Cl(1)#7	0.97	2.69	3.36(9)	126.4
Symmetry transformations used to generate equivalent atoms:				
#1 -*x*+1/2, *y*, *z*+1/2; #2 *x*+1/2, -*y*+1, *z*; #3 *x*+1/2, -*y*, *z*; #4 -*x*+1/2, *y*, *z*-1/2; #5 -*x*+1, -*y*+1, *z*+1/2; #6 *x*+1, *y*, *z*; #7 -*x*+1, -*y*, *z*+1/2.				
1-100 K				
H-bond in anions				
C(1)−H(1A)···Cl(1)#1	0.95	2.83	3.460(9)	124.9
C(2)−H(2A)···Cl(1)#1	0.95	2.86	3.467(15)	122.5
C(2)−H(2A)···Cl(4)#1	0.95	2.79	3.597(14)	142.9

C(4)−H(4A)···Cl(2)#2	0.95	2.97	3.571(9)	122.8
C(4)−H(4A)···Cl(4)#2	0.95	2.87	3.607(9)	135.7
C(7)−H(7A)···Cl(1)#3	0.95	2.90	3.548(10)	126.3
C(7)−H(7A)···Cl(3)#3	0.95	2.81	3.554(9)	135.4
C(9)−H(9A)···Cl(2)#4	0.95	2.95	3.550(16)	122.2
C(9)−H(9A)···Cl(3)#4	0.95	2.75	3.610(17)	151.0
C(10)−H(10A)···Cl(2)#4	0.95	2.82	3.481(9)	127.6
H-bonds between anions and cations				
C(11)−H(11A)···O(1)#3	0.95	2.64	3.435(15)	141.2
C(12)−H(12A)···Cl(3)#3	0.95	2.97	3.726(14)	137.6
C(13)−H(13A)···Cl(4)#5	0.95	2.80	3.694(15)	157.5
C(14)−H(14B)···Cl(2)#2	0.98	2.80	3.499(14)	129.0
C(14)−H(14C)···Cl(3)#6	0.98	2.81	3.784(15)	172.8
C(15)−H(15A)···Cl(4)#1	0.99	2.85	3.800(17)	160.2
C(16)−H(16C)···O(2)#5	0.98	2.40	3.361(13)	165.0
Symmetry transformations used to generate equivalent atoms:				
#1 -*x*+1/2, *y*, *z*+1/2; #2 *x*+1/2, -*y*+1, *z*; #3 *x*+1/2, -*y*, *z*; #4 -*x*+1/2, *y*, *z*-1/2; #5 -*x*+1, -*y*+1, *z*+1/2; #6 *x*+1, *y*, *z*.				
2-290 K				
H-bonds in anion				
C(2)−H(2)···Cl(1)#1	0.93	2.97	3.639(4)	130.5
C(2)−H(2)···Cl(4)#1	0.93	2.74	3.559(4)	147.3
C(4)−H(4)···Cl(4)#2	0.93	2.83	3.460(4)	125.6
C(7)−H(7)···Cl(3)#3	0.93	2.76	3.582(4)	148.3
C(9)−H(9)···Cl(2)#4	0.93	2.93	3.542(4)	124.3
C(9)−H(9)···Cl(3)#4	0.93	2.74	3.585(4)	151.8
H-bonds between anions and cations				
C(14)−H(14B)···Cl(4)#2	0.96	2.79	3.629(6)	146.4
C(14)−H(14C)···O(1)#5	0.96	2.52	3.260(7)	133.6
C(15)−H(15A)···Cl(4)	0.96	2.80	3.761(5)	179.0
C(15)−H(15C)···Cl(3)#5	0.96	2.80	3.752(5)	171.0
C(16)−H(16B)···Cl(2)#4	0.97	2.92	3.840(6)	158.4
C(17)−H(17C)···Cl(1)#6	0.96	2.87	3.811(6)	168.7
Symmetry transformations used to generate equivalent atoms:				
#1 -*x*+1/2, *y*+1/2, *z*; #2 *x*+1/2, -*y*+3/2, -*z*+1; #3 *x*+1/2, *y*, -*z*+1/2; #4 -*x*+1/2, *y*-1/2, *z*; #5 *x*, -*y*+3/2, *z*+1/2; #6 -*x*+1/2, -*y*+1, *z*+1/2.				
2-100 K				
H-bonds in anion				
C(2)−H(2)···Cl(1)#1	0.95	2.88	3.583(4)	131.3
C(2)−H(2)···Cl(4)#1	0.95	2.69	3.501(4)	143.5
C(4)−H(4)···Cl(4)#2	0.95	2.78	3.409(4)	124.3
C(7)−H(7)···Cl(3)#3	0.95	2.72	3.540(4)	145.1
C(9)−H(9)···Cl(2)#4	0.95	2.86	3.477(4)	123.5
C(9)−H(9)···Cl(3)#4	0.95	2.69	3.541(4)	149.7

C(10)−H(10)···Cl(2)#4	0.95	2.97	3.530(4)	119.4
H-bonds between anions and cations				
C(11)−H(11)···Cl(3)#2	0.95	2.98	3.639(4)	127.6
C(14)−H(14B)···Cl(4)#2	0.98	2.84	3.622(4)	137.3
C(14)−H(14C)···O(1)#5	0.98	2.48	3.180(5)	127.8
C(15)−H(15A)···Cl(4)	0.98	2.73	3.703(4)	172.2
C(15)−H(15B)···Cl(2)	0.98	2.95	3.659(4)	129.9
C(15)−H(15C)···Cl(3)#5	0.98	2.77	3.731(4)	166.7
C(16)−H(16A)···Cl(2)#4	0.99	2.86	3.797(4)	157.5
C(16)−H(16B)···Cl(4)	0.99	2.96	3.942(4)	171.1
C(17)−H(17C)···Cl(1)#6	0.98	2.84	3.792(4)	162.9

Symmetry transformations used to generate equivalent atoms:

#1 -*x*+1/2, *y*+1/2, *z*; #2 *x*+1/2, -*y*+3/2, -*z*+1; #3 *x*+1/2, *y*, -*z*+1/2; #4 -*x*+1/2, *y*-1/2, *z*; #5 *x*, -*y*+3/2, *z*+1/2; #6 -*x*+1/2, -*y*+1, *z*+1/2.

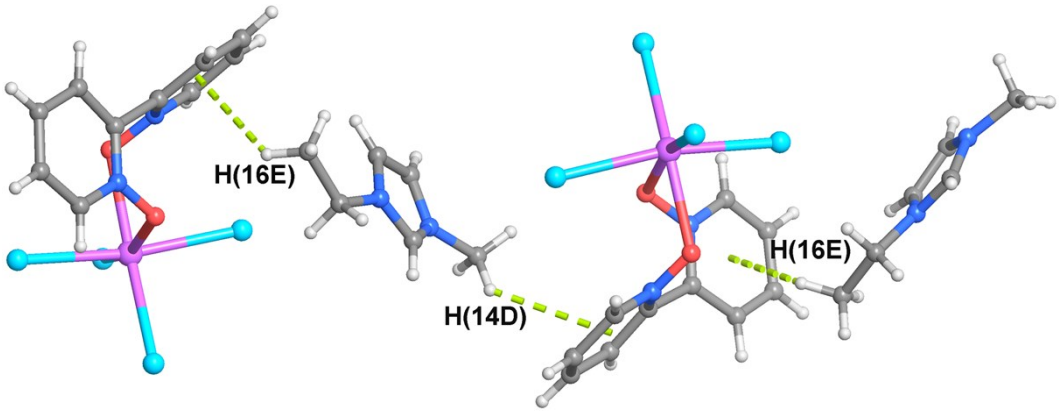

Fig. S2 The view of C−H···π interactions (lime dotted line) for **1** at 290 K between anions and cations.

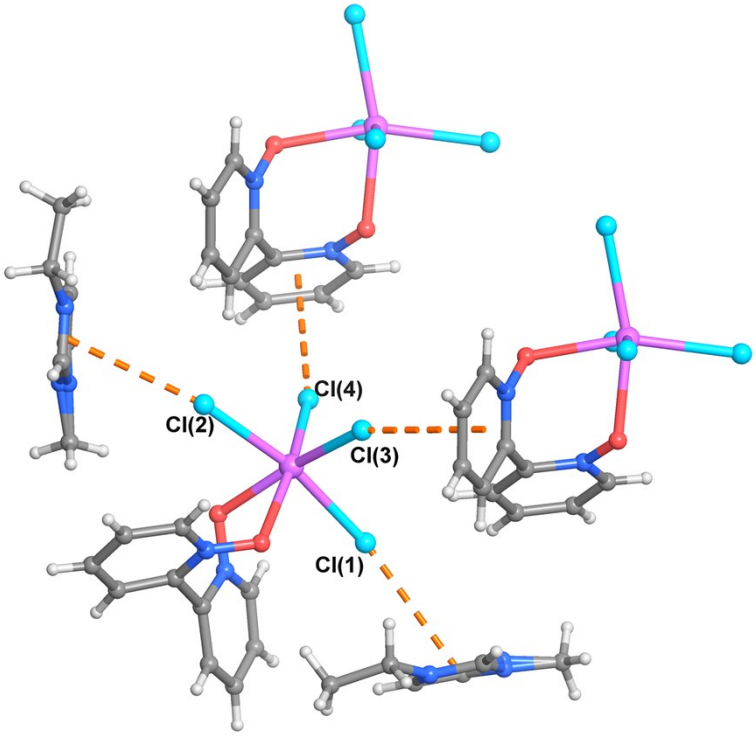

Fig. S3 The view of anion···π interactions (orange dotted line) for **1** at 290 K between anions and cations and between anions and cations.

Table S4. Selected weak interaction data for **1** at 290 K.

Y−X(I)···Cg(J)	ARU(J)	X···Cg(Å)	<Y−X···Cg(°)	Y···Cg(Å)	Y−X, Pi
C−H···π interactions					
C(14B)−H(14D)→Cg(3)	4565.02	2.98	130	3.68(11)	61.00
C(16B)−H(16E)→Cg(4)	2655.02	2.79	129	3.48(7)	35.00
anion···π interactions					
Bi(1)−Cl(1)→Cg(1)	2654.01	3.723(10)	162.58(19)	6.302(10)	51.67
Bi(1)−Cl(1)→Cg(2)	2654.01	3.755(17)	162.4(3)	6.331(16)	48.25
Bi(1)−Cl(2)→Cg(1)	4465.01	3.631(10)	153.55(19)	6.157(10)	52.33
Bi(1)−Cl(2)→Cg(2)	4465.01	3.599(17)	153.6(3)	6.127(16)	48.98
Bi(1)−Cl(3)→Cg(3)	4455.02	3.662(7)	158.98(17)	6.252(6)	55.71
Bi(1)−Cl(4)→Cg(4)	4465.02	3.649(7)	159.35(17)	6.252(7)	55.65

Cg(1): N(3)→C(11)→C(12)→N(4)→C(13). Cg(2): N(4)→C(12)→C(11)→N(3B)→C(13). Cg(3): N(1)→C(1)→C(2)→C(3)→C(4)→C(5). Cg(4): N(2)→C(6)→C(7)→C(8)→C(9)→C(10). [4565] = 1/2+*x*, 1-*y*, *z*. [2655] = 1-*x*, -*y*, 1/2+*z*. [2654] = 1-*x*, -*y*, -1/2+*z*. [4465] = -1/2+*x*, 1-*y*, *z*. [4455] = -1/2+*x*, -*y*, *z*. [4465] = -1/2+*x*, 1-*y*, *z*.

Notably, the ethyl chain in $[Emim]^+$ of **1** follows statistical distribution at 290 K. The disorder in cation for **1** leads to additional weak interactions (Table S4):

1) **anion···π interactions:** another two anion···π interactions exist between Cl atoms (Cl(1) and Cl(2)) and imidazole ring.
2) **C−H···π interactions: 1** also possesses additional C−H···π interactions with the distance of 2.98 and 2.79 Å between two pyridine rings from anion and the alkyl chain in cation (Fig. S2).

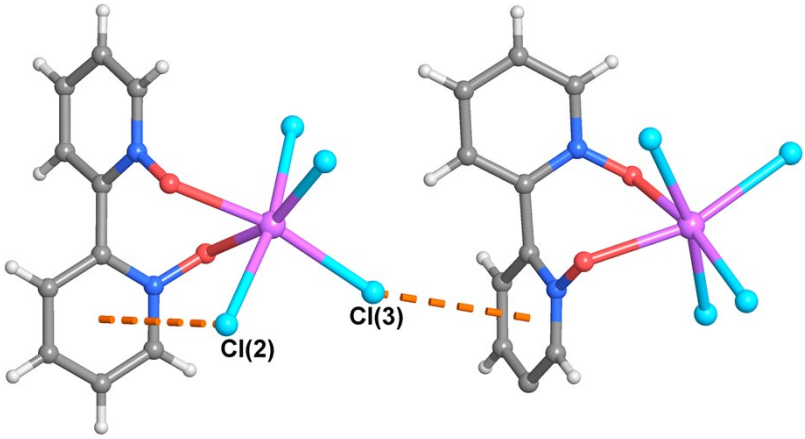

Fig. S4 The view of anion···π interactions (orange dotted line) for **2** at 290 K in the anionic part.

Table S5. Selected weak interaction data for **2** at 290 K.

Y−X(I)···Cg(J)	ARU(J)	X···Cg(Å)	<Y−X···Cg(°)	Y···Cg(Å)	Y−X, Pi
anion···π interactions					
Bi(1)−Cl(2)→Cg(1)	1555.01	3.741(2)	82.62(4)	4.3185(16)	25.03
Bi(1)−Cl(3)→Cg(1)	6455.01	3.5707(19)	156.38(4)	6.1098(16)	54.57

Cg(1): N(1)→C(1)→C(2)→C(3)→C(4)→C(5). Cg(2): N(2)→C(6)→C(7)→C(8)→C(9)→C(10). Cg(3): N(3)→C(11)→C(12)→N(4)→C(13). [1555] = x, y, z. [6455] = -1/2+x, y, 1/2-z.

Table S6. Selected weak interaction data for **1** at 100 K.

Y−X(I)···Cg(J)	ARU(J)	X···Cg(Å)	<Y−X···Cg(°)	Y···Cg(Å)	Y−X, Pi
anion···π interactions					
Bi(1)−Cl(1)→Cg(3)	2654.02	3.557(6)	161.09(13)	6.133(6)	52.96
Bi(1)−Cl(2)→Cg(3)	4465.02	3.686(6)	157.54(13)	6.243(6)	53.28
Bi(1)−Cl(3)→Cg(1)	4455.01	3.565(5)	157.30(12)	6.163(4)	55.74
Bi(1)−Cl(4)→Cg(2)	4465.01	3.553(5)	158.17(12)	6.164(5)	54.65

Cg(1): N(1)→C(1)→C(2)→C(3)→C(4)→C(5). Cg(2): N(2)→C(6)→C(7)→C(8)→C(9)→C(10). Cg(3): N(3)→C(11)→C(12)→N(4)→C(13). [2654] = 1-x, -y, -1/2+z. [4465] = -1/2+x, 1-y, z. [4455] = -1/2+x, -y, z. [4465] = -1/2+x, 1-y, z.

Table S7. Selected weak interaction data for **2** at 100 K.

Y−X(I)···Cg(J)	ARU(J)	X···Cg(Å)	<Y−X···Cg(°)	Y···Cg(Å)	Y−X, Pi
anion···π interactions					
Bi(1)−Cl(2)→Cg(1)	1555.01	3.6689(16)	83.56(3)	4.3037(13)	24.13
Bi(1)−Cl(3)→Cg(1)	6455.01	3.4847(16)	156.08(4)	6.0362(14)	54.80

Cg(1): N(1)→C(1)→C(2)→C(3)→C(4)→C(5). Cg(2): N(2)→C(6)→C(7)→C(8)→C(9)→C(10). Cg(3): N(3)→C(11)→C(12)→N(4)→C(13). [1555] = *x*, *y*, *z*. [6455] = -1/2+*x*, *y*, 1/2-*z*.

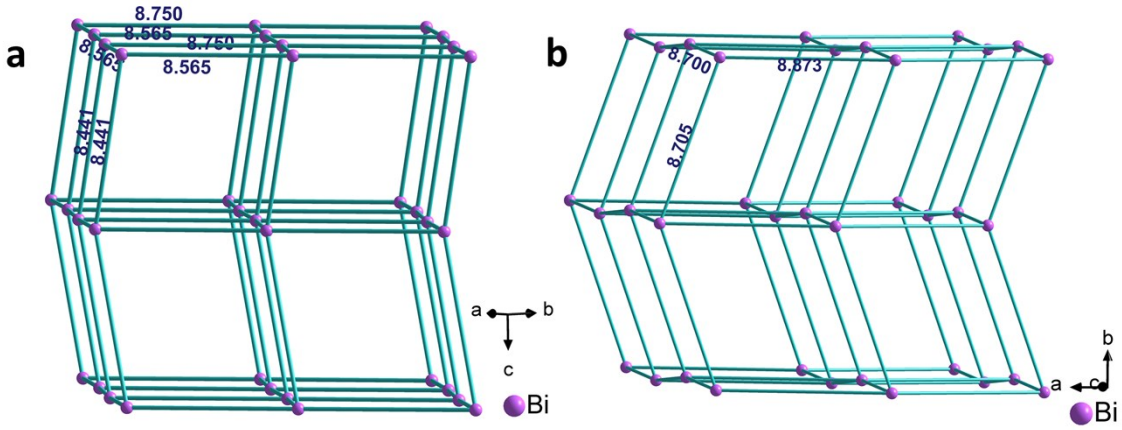

Fig. S5 Topological structures of **1** (a) and **2** (b) created by linking adjacent Bi atoms. Both compounds exhibit **pcu** topological structure. The distances of adjacent Bi atoms are 8.441, 8.565, 8.750 for **1** and 8.700, 8.705, 8.873 for **2**.

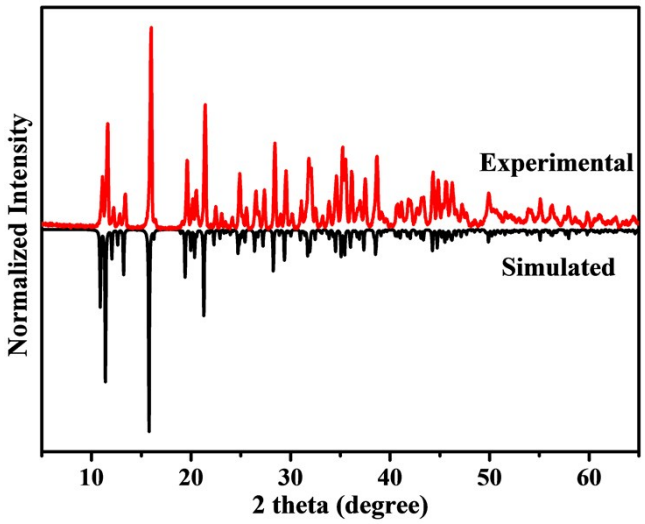

Fig. S6 PXRD patterns of **1**.

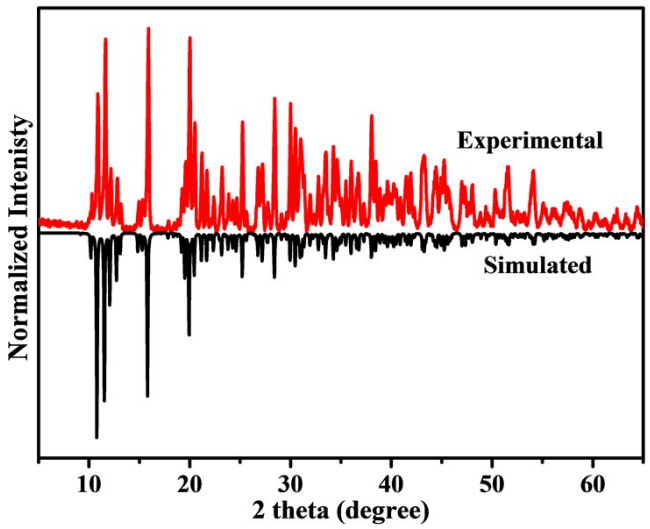

Fig. S7 PXRD patterns of **2**.

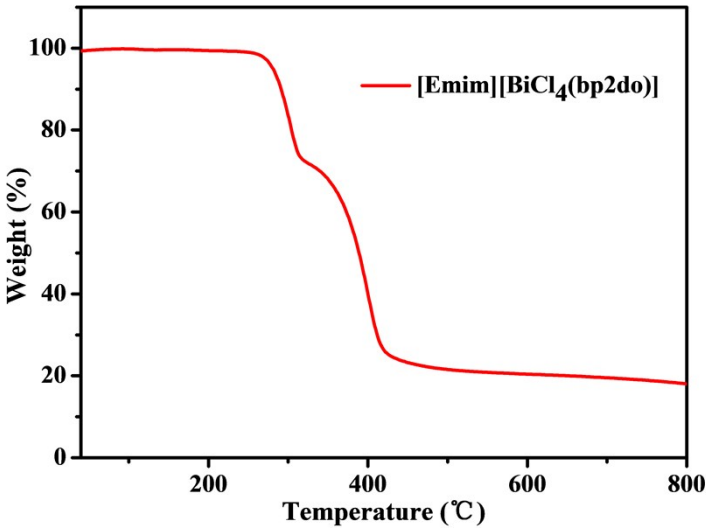

Fig. S8 TG curve of **1**.

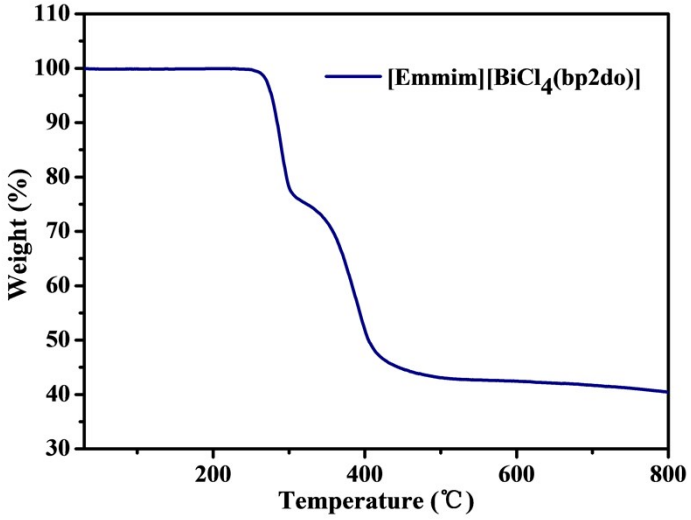

Fig. S9 TG curve of **2**.

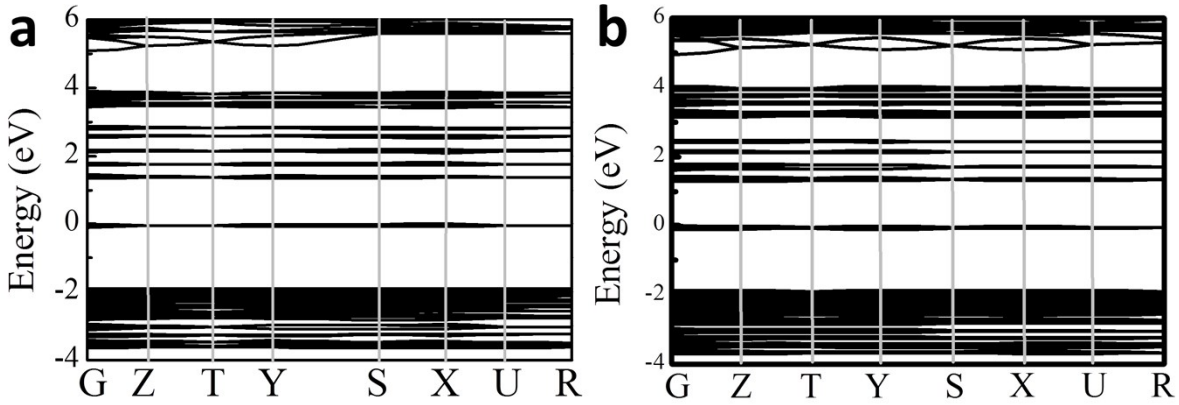

Fig. S10 The electronic band structure of **1** (a) and **2** (b). The calculated bandgap is 1.332 for **1** and 1.281 eV for **2**.

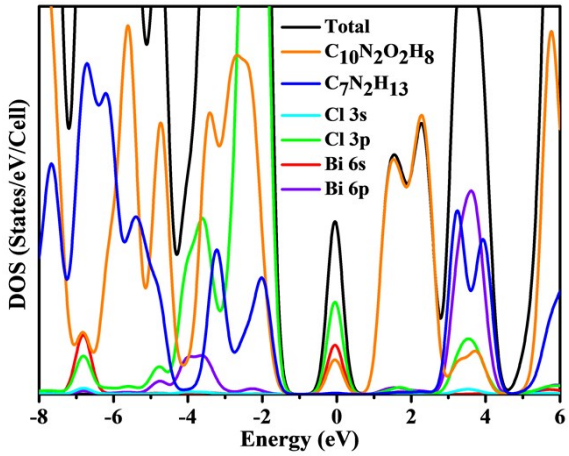

Fig. S11 Density of states (DOSs) for **2**. The $C_{10}N_2O_2H_8$ represents the bp2do organic ligand and the $C_7N_2H_{13}$ represents the $[Emmim]^+$ cation.

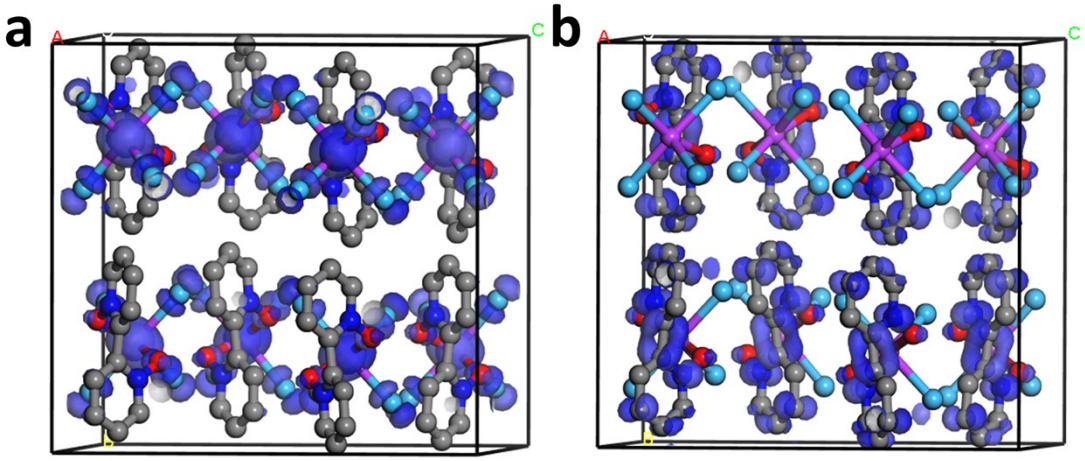

Fig. S12 The molecular orbitals of **2** showing the highest occupied molecular orbital (a, HOMO) and the lowest occupied molecular orbital (b, LUMO). The isosurface values are 0.02.

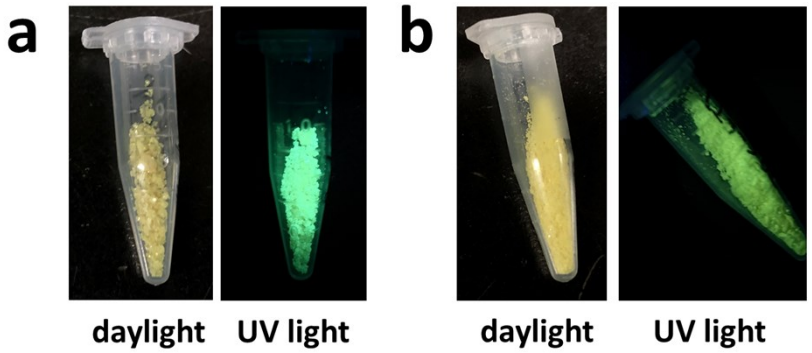

Fig. S13 (a) Photographs of **1** under daylight (left) and UV light (right). (b) Photographs of **2** under daylight (left) and UV light (right).

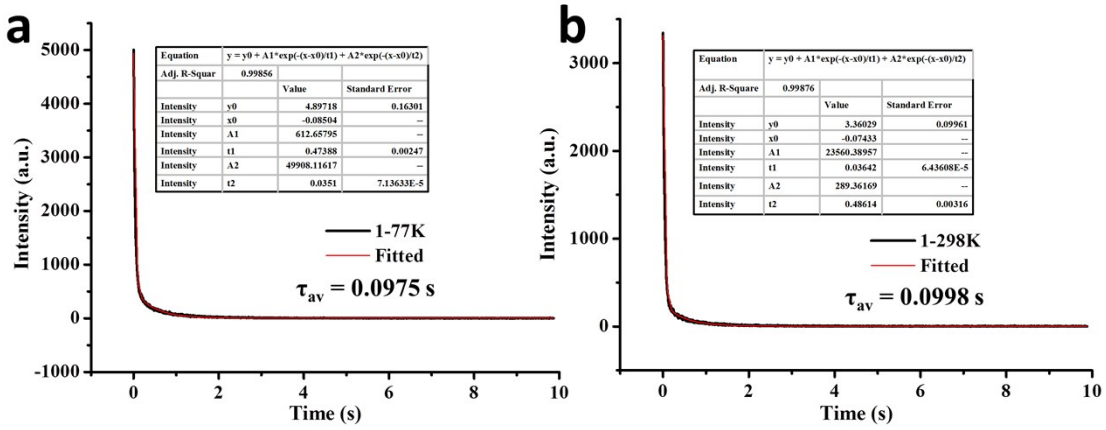

Fig. S14 PL decay spectra of **1** at 77 K (a) and 298 K (b). The data could be fitted well by bi-exponential function. The average lifetime is 0.0975 s at 77 K (τ1 = 0.474 s, 14.20%; τ2 = 0.0351 s, 85.80%) and 0.0998 s at 298 K (τ1 = 0.0364 s, 85.90%; τ2 = 0.486 s, 14.10%), respectively.

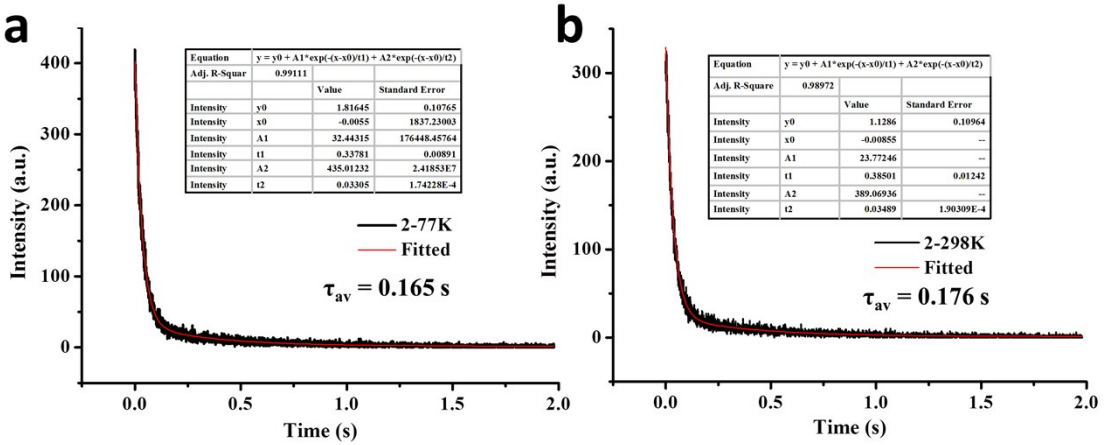

Fig. S15 PL decay spectra of **2** at 77 K (a) and 298 K (b). The data could be fitted well by bi-exponential function. The average lifetime is 0.165 s at 77 K (τ1 = 0.338 s, 43.30%; τ2 = 0.0331 s, 56.70%) and 0.176 s at 298 K (τ1 = 0.385 s, 40.30%; τ2 = 0.0349 s, 59.70%), respectively.

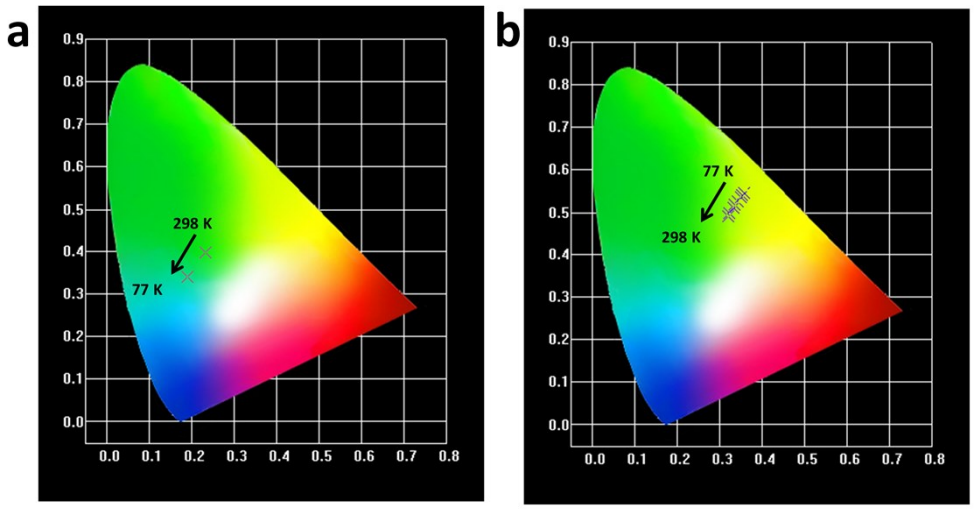

Fig. S16 The temperature-dependent CIE (1931) chromaticity coordinates of **1** (a) and **2** (b) from 77 K to 298 K.

Table S8 The distortion of bismuth-chloride/oxygen bonds and angles for **1** and **2** at 290 K and 100 K.

Compound	*D*	λ_{oct}	σ^2
1-290 K	0.04929	1.0219	63.88
1-100 K	0.05552	1.0246	69.64
2-290 K	0.04414	1.0187	57.38
2-100 K	0.04851	1.0206	62.55

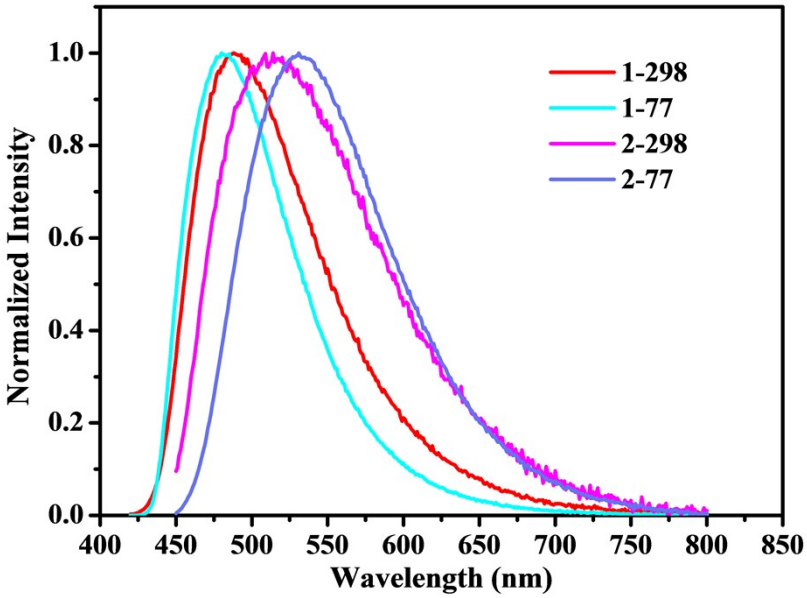

Fig. S17 Normalized emission spectra of **1** and **2** at 290 K and 77 K. The excitation wavelength is 410 nm for **1** and 430 nm for **2**.

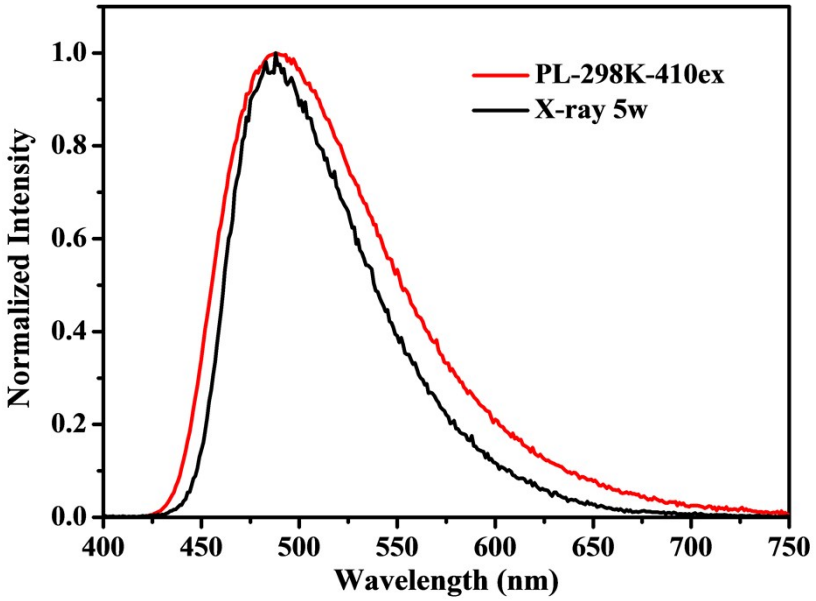

Fig. S18 Comparison of normalized PL spectra for **1** under different excited resources at RT. The black solid line is under X-ray excitation while the red solid line is under 410 nm UV excitation.

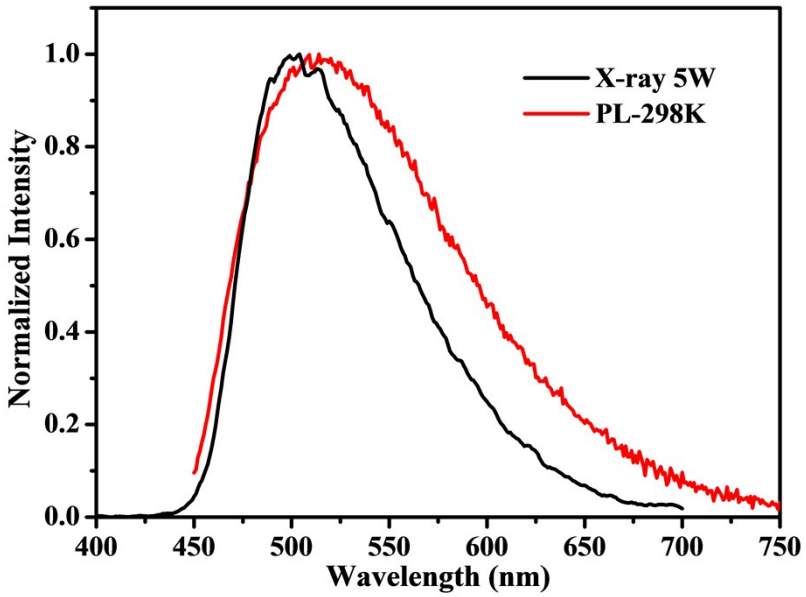

Fig. S19 Comparison of normalized PL spectra for **2** under different excited resources at RT. The black solid line is under X-ray excitation while the red solid line is under 430 nm UV excitation.

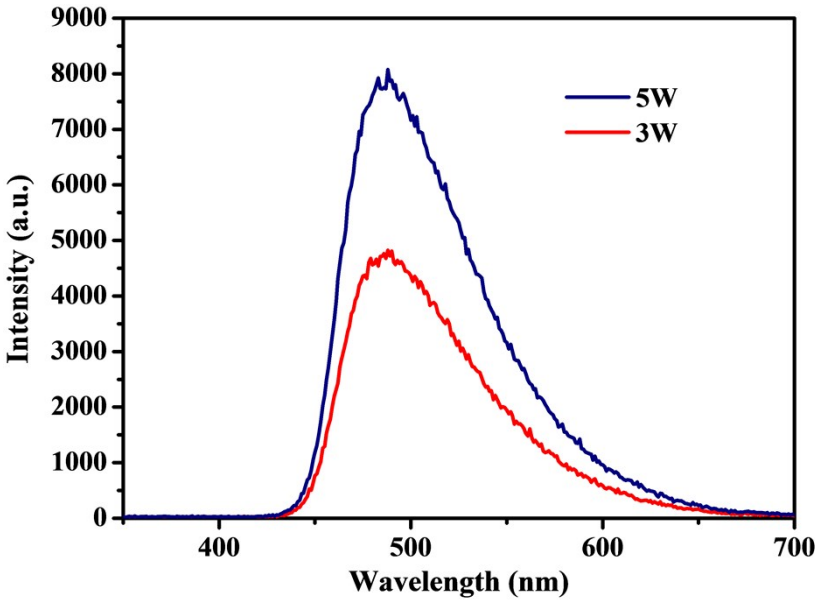

Fig. S20 X-ray excited PL spectra of **1** at RT. Mo anode was used as X-ray resource. The power is 3 W (50 kV, 60 μA) in red solid line and 5 W (50 kV, 100 μA) in blue solid line.

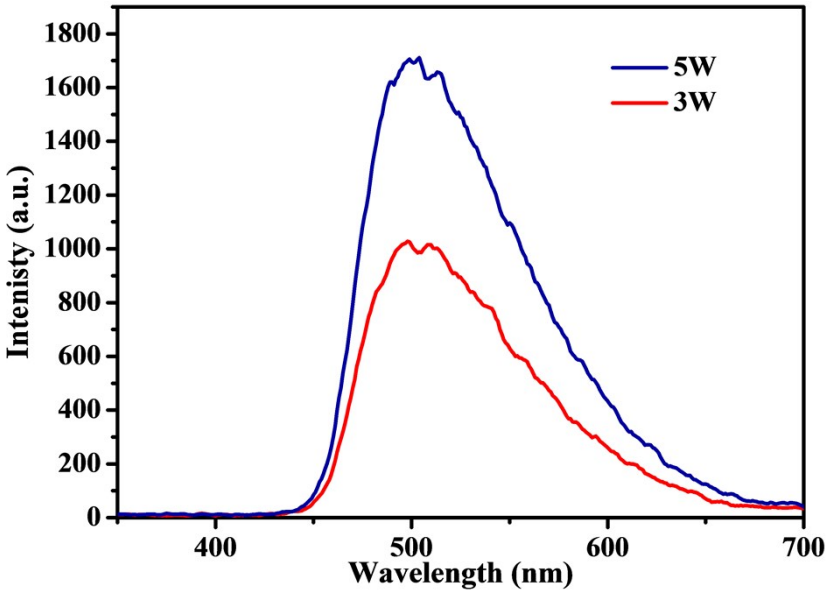

Fig. S21 X-ray excited PL spectra of **2** at RT. Mo anode was used as X-ray resource. The power is 3 W (50 kV, 60 μA) in red solid line and 5 W (50 kV, 100 μA) in blue solid line.